Electronic Supplementary Material (ESI) for Materials Chemistry Frontiers.

Supporting Information

In-situ Growth of Tubular MoS_2 Membrane on Ceramic Tube with Improved Organic Solvent Nanofiltration Performances

Tongtong Liu[a], Zhenping Qin[a], Qiaohong Liu[a,*], Xuejian Li[b], Yue Liu[a], Quan-Fu An[a], Hongxia Guo[b,*]

[a]*Beijing Key Laboratory for Green Catalysis and Separation, Department of Environmental and Chemical Engineering, Beijing University of Technology, 100124 Beijing, P. R. China*

[b]*Key Laboratory of Advanced Functional Materials of the Ministry of Education, College of Materials Science and Engineering, Beijing University of Technology, 100124 Beijing, P. R. China*

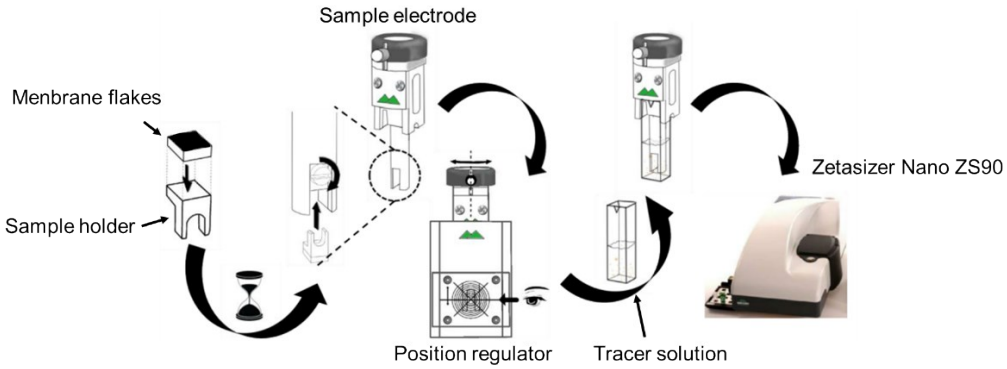

Figure S1. Schematic diagram of Zeta potential test on tubular membrane surface (pH of tracer solution is 7).

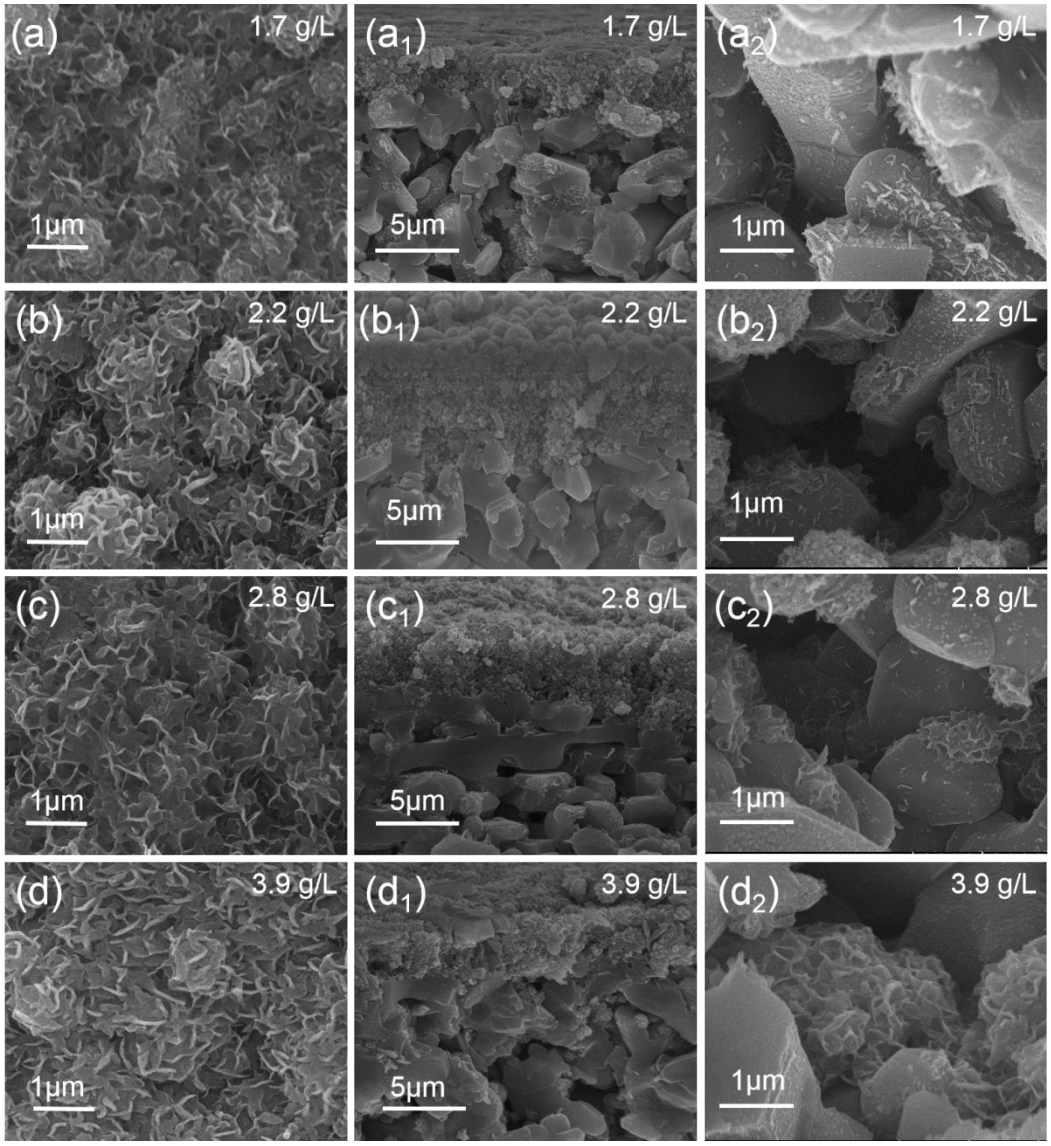

Figure S2. (a-d):SEM images of MoS_2 tubular ceramic membranes obtained with varying precursor solution from 1.7 $g{\cdot}L^{-1}$ to 3.9 $g{\cdot}L^{-1}$; (a_1-d_1): cross-sectional SEM image of MoS_2 tubular ceramic membranes with varying precursor solution, (a_2-d_2) indicated the amplified view of a_1-d_1 correspondently.

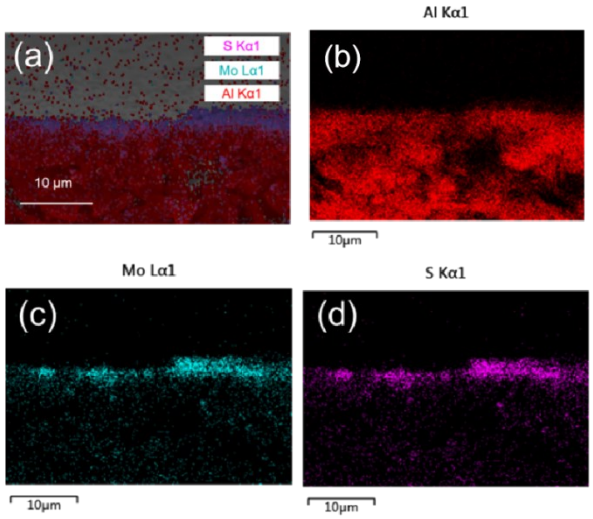

Figure S3. Energy Dispersive Spectrometer (EDS) analyses on the cross-section of the MoS_2 tubular ceramic membrane.

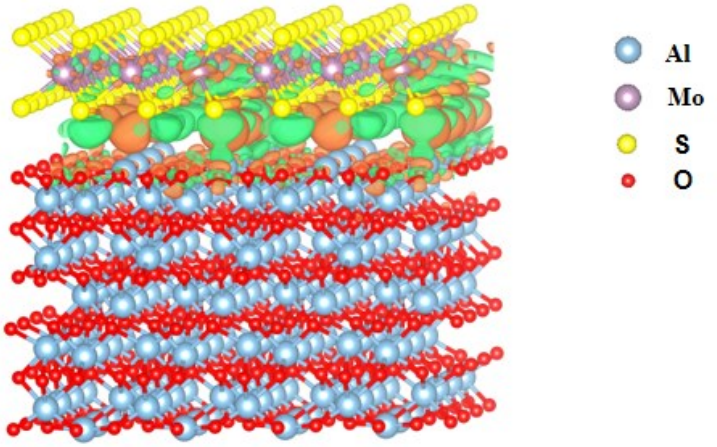

Figure S4. Deformation electron density, as the electron density difference between non-interacting and interacting systems, indicated the charge transfer process between MoS_2 layer and Al_2O_3 substrate using density functional theory.

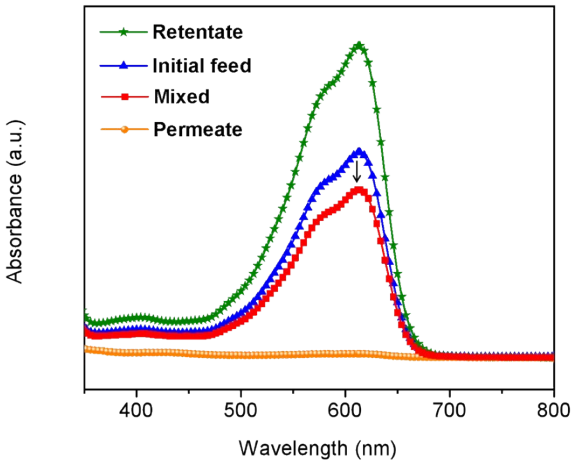

Figure S5. Dynamic adsorption experiment of MoS_2 tubular ceramic membrane (EB-MeOH concentration of initial feed: 0.01 g·L^{-1}; Operating pressure: 0.2 MPa. Mixed: the mixture of permeate and retention solution after the membrane runs stably in EB-MeOH)

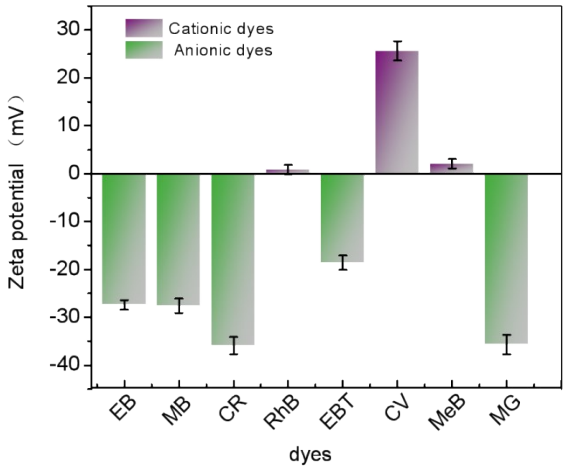

Figure S6. Zeta potential of different dyes in MeOH (Concentration: 0.1 g L^{-1}, pH=6).

Table S1. Comparison of the separation performance of the MoS_2 tubular ceramic membrane *versus* other reported membranes in methanol media.

Membrane	Dyes	Molecular weight (g mol^{-1})	Charge	Rejection (%)	Flux (L m^{-2} h^{-1} MPa^{-1})	Reference
MoS_2	Evans blue	960.8	−	98.1	403.1	This work
ZIF-8@GO/PEI	Methyl blue	799.8	−	99	61	[1]
MPD-TMC (0.4% NaOH) (with DMF mortification)	Acid fuchsin	585.5	−	90.2	263	[2]
MPD-TMC(without activation)	Methyl orange	327.33	+	98.9	137.3[a]	[3]
PAR-BHPF/PI	Rose bengal	1017.6	−	99	80	[4]
Cyclodextrins-terephthaloyl chloride	Methyl orange	327.3	+	91	94	[5]
PPSU	Rose Bengal	1017.6	−	66	18	[6]
Highly-laminated GO	Methylene Blue	319.9	+	99.9	90[a]	[7]
PBI/HPBI	Methylene blue	319.9	+	99.2	26	[8]
TETA-TFN	Crystal violet	408.0	−	92	278	[9]
rGO- TMPyP1.3	Evans blue	960.8	−	93	130	[10]
HLGO	Brilliant blue	826	−	~100	75	[7]
Porphyrin/MPD	Brilliant blue	826	−	59	325	[11]

GO/BA	Acid fuchsin	585.5	_	95	35	[12]
S-rGO	Acid fuchsin	585.5	_	70.1	780	[13]

[a] The MeOH permeance data were obtained from pure MeOH rather than the separation of dyes-MeOH mixtures.

References

[1] H. Yang, N. Wang, L. Wang, H.X. Liu, Q.F. An, S. Ji, Vacuum-Assisted Assembly of ZIF-8@GO Composite Membranes on Ceramic Tube with Enhanced Organic Solvent Nanofiltration Performance, *J. Membr. Sci.* 2018, **545**, 158-166.

[2] L. Xia, J. Ren, M. Weyd, J.R. McCutcheon, Ceramic-Supported Thin Film Composite Membrane for Organic Solvent Nanofiltration, *J. Membr. Sci.* 2018, **563**, 857-863.

[3] S. Karan, Z. Jiang, A.G. Livingston, Sub-10nm Polyamide Nanofilms with Ultrafast Solvent Transport for Molecular Separation, *Science* 2015, **348**, 1347-1351.

[4] M.F. Jimenez-Solomon, Q. Song, K.E. Jelfs, M. Munoz-Ibanez, A.G. Livingston, Polymer Nanofilms with Enhanced Microporosity by Interfacial Polymerization, *Nat. Mater.* 2016, **15**, 760-767.

[5] L.F. Villalobos, T. Huang, K.V. Peinemann, Cyclodextrin Films with Fast Solvent Transport and Shape-Selective Permeability, Adv. Mater. 2017, **29**, 1606641.

[6] S. Darvishmanesh, J.C. Jansen, F. Tasselli, E. Tocci, P. Luis, J. Degrève, E. Drioli, B. Van der Bruggen, Novel Polyphenylsulfone Membrane for Potential Use in Solvent Nanofiltration, *J. Membr. Sci.* 2011, **379**, 60-68.

[7] Q. Yang, Y. Su, C. Chi, C.T. Cherian, K. Huang, V.G. Kravets, F.C. Wang, J.C. Zhang, A. Pratt, A.N. Grigorenko, Ultrathin Graphene-Based Membrane with Precise Molecular Sieving and Ultrafast Solvent Permeation, *Nat. Mater.* 2017, **16**, 1198-1202.

[8] L. Shao, X. Cheng, Z. Wang, J. Ma, Z. Guo, Tuning the Performance of Polypyrrole-Based Solvent-Resistant Composite Nanofiltration Membranes by Optimizing Polymerization Conditions and Incorporating Graphene Oxide, *J. Membr. Sci.* 2014, **452**, 82-89.

[9] I. Soroko, A. Livingston, Impact of TiO_2 Nanoparticles on Morphology and Performance of Crosslinked Polyimide Organic Solvent Nanofiltration (OSN) Membranes, *J. Membr. Sci.* 2009, **343**, 189-198.

[10] T. Gao, L. Huang, C. Li, G. Xu, G. Shi, Graphene Membranes with Tuneable Nanochannels by Intercalating Self-Assembled Porphyrin Molecules for Organic Solvent Nanofiltration, *Carbon*, 2017, **124**, 263-270.

[11] P.H.H. Duong, D.H. Anjum, K.-V. Peinemann, S.P. Nunes, Thin Porphyrin Composite Membranes with Enhanced Organic Solvent Transport, *J. Membr. Sci.* 2018, **563**, 684-693.

[12] T. Gao, H. Wu, L. Tao, L. Qu, C. Li, Enhanced Stability and Separation Efficiency of Graphene Oxide Membranes in Organic Solvent Nanofiltration, *J. Mater. Chem. A* 2018, **6**, 19563-19569.

[13] L. Huang, J. Chen, T. Gao, M. Zhang, Y. Li, L. Dai, L. Qu, G. Shi, Reduced Graphene Oxide Membranes for Ultrafast Organic Solvent Nanofiltration, *Adv. Mater.* 2016, **28**, 8669-8674.